

Springer Climate

Song Yang · Renguang Wu ·  
Maoqiu Jian · Jian Huang ·  
Xiaoming Hu · Ziqian Wang ·  
Xingwen Jiang

# Climate Change in Southeast Asia and Surrounding Areas




Science Press  
Beijing



Springer

# Springer Climate

## Series Editor

John Dodson , Institute of Earth Environment, Chinese Academy of Sciences,  
Xian, Shaanxi, China

Springer Climate is an interdisciplinary book series dedicated to climate research. This includes climatology, climate change impacts, climate change management, climate change policy, regional climate studies, climate monitoring and modeling, palaeoclimatology etc. The series publishes high quality research for scientists, researchers, students and policy makers. An author/editor questionnaire, instructions for authors and a book proposal form can be obtained from the Publishing Editor. **Now indexed in Scopus® !**

More information about this series at <http://www.springer.com/series/11741>

Song Yang · Renguang Wu · Maoqiu Jian ·  
Jian Huang · Xiaoming Hu · Ziqian Wang ·  
Xingwen Jiang

# Climate Change in Southeast Asia and Surrounding Areas

 Science Press  
Beijing

 Springer

See next page

ISSN 2352-0698

Springer Climate

ISBN 978-981-15-8224-0

<https://doi.org/10.1007/978-981-15-8225-7>

ISSN 2352-0701 (electronic)

ISBN 978-981-15-8225-7 (eBook)

Jointly published with Science Press.

The print edition is not for sale in China (Mainland). Customers from China (Mainland) please order the print book from Science Press

© Science Press and Springer Nature Singapore Pte Ltd. 2021

This work is subject to copyright. All rights are reserved by the Publishers, whether the whole or part of the material is concerned, specifically the rights of translation, reprinting, reuse of illustrations, recitation, broadcasting, reproduction on microfilms or in any other physical way, and transmission or information storage and retrieval, electronic adaptation, computer software, or by similar or dissimilar methodology now known or hereafter developed.

The use of general descriptive names, registered names, trademarks, service marks, etc. in this publication does not imply, even in the absence of a specific statement, that such names are exempt from the relevant protective laws and regulations and therefore free for general use.

The publishers, the authors, and the editors are safe to assume that the advice and information in this book are believed to be true and accurate at the date of publication. Neither the publishers nor the authors or the editors give a warranty, express or implied, with respect to the material contained herein or for any errors or omissions that may have been made. The publishers remain neutral with regard to jurisdictional claims in published maps and institutional affiliations.

This Springer imprint is published by the registered company Springer Nature Singapore Pte Ltd.

The registered company address is: 152 Beach Road, #21-01/04 Gateway East, Singapore 189721, Singapore

Song Yang  
School of Atmospheric Sciences  
Sun Yat-sen University  
Zhuhai, Guangdong, China

Guangdong Province Key Laboratory  
for Climate Change and Natural  
Disaster Studies  
Zhuhai, China

Southern Marine Science and Engineering  
Guangdong Laboratory (Zhuhai)  
Zhuhai, China

Maoqiu Jian  
School of Atmospheric Sciences  
Sun Yat-sen University  
Zhuhai, Guangdong, China

Guangdong Province Key Laboratory  
for Climate Change and Natural  
Disaster Studies  
Zhuhai, China

Southern Marine Science and Engineering  
Guangdong Laboratory (Zhuhai)  
Zhuhai, China

Xiaoming Hu  
School of Atmospheric Sciences  
Sun Yat-sen University  
Zhuhai, Guangdong, China

Guangdong Province Key Laboratory  
for Climate Change and Natural  
Disaster Studies  
Zhuhai, China

Southern Marine Science and Engineering  
Guangdong Laboratory (Zhuhai)  
Zhuhai, China

Xingwen Jiang  
Institute of Plateau Meteorology  
China Meteorological Administration  
Chengdu, Sichuan, China

Renguang Wu  
School of Earth Sciences  
Zhejiang University  
Hangzhou, Zhejiang, China

Jian Huang  
Institute of Tropical and Marine  
Meteorology  
China Meteorological Administration  
Guangzhou, Guangdong, China

Ziqian Wang  
School of Atmospheric Sciences  
Sun Yat-sen University  
Zhuhai, Guangdong, China

Guangdong Province Key Laboratory  
for Climate Change and Natural  
Disaster Studies  
Zhuhai, China

Southern Marine Science and Engineering  
Guangdong Laboratory (Zhuhai)  
Zhuhai, China

# Contents

<b>1</b>	<b>Introduction</b> .....	1
	References .....	6
<b>2</b>	<b>Characteristics of the Spring–Summer Atmospheric Circulation Transition Over the South China Sea and Its Surrounding Regions and Their Responses to Global Warming</b> .....	7
2.1	Characteristics of the Transition Over the SCS and Its Surrounding Regions .....	8
2.1.1	Characteristics of the Transition .....	9
2.1.2	Physical Processes of the Transition .....	14
2.2	Interannual Variation of Net Heat Flux Over the Indian Ocean and the Western Pacific Ocean During the Transition .....	24
2.3	Impact of Intraseasonal Oscillation on SCSSM Onset .....	28
2.3.1	Relationship Between SCSSM Onset and MJO Activity .....	31
2.3.2	Physical Process Behind MJO Impact on SCSSM Onset .....	32
2.3.3	Synergy Between MJO and Tropical SST .....	35
2.4	Precursory Signals for SCSSM Onset .....	38
2.4.1	Multi-time-scale Characteristics of SCSSM Onset Date ...	39
2.4.2	Precursory SST Signals for Interannual Variation and Interdecadal Change of SCSSM Onset .....	40
2.4.3	Asymmetry Between the Central–Eastern Equatorial Pacific SSTA and SCSSM Onset .....	42
2.5	Responses of Subtropical Highs to Global Warming .....	44
2.5.1	Model, Data, and Method .....	45
2.5.2	Response of the WNPSH to Global Warming .....	46
2.5.3	Responses of Subtropical Anticyclones to Global Warming .....	56

2.6	Response of SCSSM Onset to Global Warming . . . . .	64
2.6.1	Models, Data, and Method . . . . .	65
2.6.2	SCSSM Onset in CMIP5 Historical Experiments . . . . .	65
2.6.3	Response of SCSSM Onset to Global Warming . . . . .	67
2.7	Summary . . . . .	72
	References . . . . .	75
<b>3</b>	<b>Air–Sea Interactions and Climate Variability Over the South China Sea and the Adjacent Regions . . . . .</b>	<b>81</b>
3.1	Air–Sea Interactions on Different Time Scales . . . . .	82
3.1.1	Intraseasonal Air–Sea Interactions . . . . .	83
3.1.2	Interannual Air–Sea Interactions . . . . .	92
3.2	Processes for Interannual Variability of Rainfall Over the South China Sea . . . . .	97
3.2.1	Interannual Variations of Summer Rainfall in the South China Sea . . . . .	98
3.2.2	Interannual Variations Of the South China Sea Rainfall During the Spring-To-Summer Transition . . . . .	102
3.2.3	Influence Of Local Air–Sea Interaction on the South China Sea Climate During the Spring-to-Summer Transition . . . . .	104
3.3	Interdecadal Variation . . . . .	109
3.3.1	Interdecadal Variability Of Early Summer Monsoon Rainfall Over South China In Association With the Pacific Decadal Oscillation . . . . .	109
3.3.2	Interdecadal Modulation of ENSO-Related Spring Rainfall Over South China by the Pacific Decadal Oscillation . . . . .	112
3.4	Cross-Scale Relation . . . . .	120
3.4.1	Interannual Variation of the Intensity of the Summer ISO Over the Tropical Western North Pacific . . . . .	120
3.4.2	The Change of the Intensity of the ISOs Over the Tropical Indo-Pacific Region With the Phase of ENSO . . . . .	123
3.4.3	Feedback of ISOs on Seasonal Mean SST Anomalies in the Tropical Western North Pacific . . . . .	125
3.4.4	Influence of ISOs on Interdecadal Change . . . . .	128
3.4.5	Influence of Interannual Variation on Synoptic Disturbances . . . . .	129
3.5	Summary . . . . .	131
	References . . . . .	133



**4 Land–Atmosphere Interaction and Climate Variability in Southeast Asia and Its Surrounding Area** . . . . . 139

4.1 Field Observations of Typical Underlying Land-Surface Process and Relevant Theoretical Analysis . . . . . 140

4.1.1 Field Observations of Typical Underlying Surface in the South China . . . . . 140

4.1.2 Data Processing Method . . . . . 142

4.1.3 Analysis on Characteristics of Typical Underlying Surface Land–Atmosphere Interaction in South China and Its Surrounding Area . . . . . 148

4.2 Influence of Land–Atmosphere Interaction on Climate Change of the South China Sea and Its Surrounding Areas as a Response to Global Climate Change . . . . . 168

4.2.1 Correction, Optimization, and Improvement of Important Land-Surface Process Parameters of the Typical Underlying Surfaces in the South China Sea and the Surrounding Area . . . . . 169

4.2.2 Influences of Land–Atmosphere Interaction on Spring and Summer Climate Variability in Southeast Asia and Its Surrounding Areas, and Mechanism . . . . . 175

4.3 Land–Air Interaction and Climate Variation in Southeast Asia and Its Surrounding Areas . . . . . 184

4.3.1 Relationships Among Surface Energy, Water Balance Characteristics, and Regional Climate Anomalies of Typical Underlying Surface in Southeast Asia . . . . . 184

4.3.2 Physical Process of Soil Moisture Affecting Summer Precipitation . . . . . 190

4.3.3 Effect of Soil Moisture on the South China Sea Summer Monsoon . . . . . 196

References . . . . . 200

**5 Effects of the Tibetan Plateau on Climate** . . . . . 205

5.1 Introduction . . . . . 205

5.2 Effects of the TP Summer Heating on Climate in Regional Models . . . . . 206

5.2.1 Models and Experimental Design . . . . . 206

5.2.2 Two Types of TP Heating and Their Interactions . . . . . 208

5.2.3 Effects on Meridional Circulation and on Temperature and Circulation in the Upper Troposphere . . . . . 211

5.2.4 TP Heating and Potential Vorticity Forcing Near the Tropopause . . . . . 214

5.2.5 Potential Regulation by Tropical Air-Sea Coupling . . . . . 216

5.3	Key Effect of TP on Eurasian Teleconnection . . . . .	219
5.3.1	Data and Model . . . . .	220
5.3.2	The Bridge Effect of TP on Eurasian Teleconnection . . . . .	220
5.3.3	Direct Impact of TP Heating on East China Summer Rainfall in AGCM Experiments . . . . .	224
5.4	Thermal Effect of TP on Climate Variation Over the Upstream Regions . . . . .	225
5.4.1	Data, Model, and Experimental Design . . . . .	227
5.4.2	Impact of TP Surface Heating on Climate Variation Over West Asia, North Africa, South Europe, and the North Atlantic . . . . .	228
5.4.3	Conclusions and Discussion . . . . .	235
5.5	Climate Effect of SAH Variability Over TP . . . . .	236
5.5.1	Zonal Shift of SAH and Its Relationship with Asian Summer Monsoon Rainfall . . . . .	236
5.5.2	Relationship with the ISM and EASM Rainfall . . . . .	237
5.5.3	Impact of ISM Rainfall on the Zonal Shift of SAH . . . . .	239
5.5.4	Impact of Zonal Displacement of SAH on the Summer Rainfall Over China . . . . .	242
5.5.5	Impact of YRV Rainfall on the Zonal Shift of SAH . . . . .	243
5.5.6	Conclusions and Discussion . . . . .	247
	References . . . . .	248
<b>6</b>	<b>Feedback Attributions of Climate Changes Over the Globe and Over Southeast Asia and Its Adjacent Regions . . . . .</b>	<b>253</b>
6.1	Overview . . . . .	253
6.2	Climate Response-Feedback Analysis Method . . . . .	255
6.3	Attribution of Decadal Climate Difference Between 2002–13 and 1984–95 . . . . .	259
6.4	Feedback Attribution of Interannual Variability . . . . .	261
6.4.1	Attribution of the Distinct Spatial Patterns of SST Anomalies for Two Types of El Niño . . . . .	261
6.4.2	Variations of Dominant Modes of the East Asian Winter Monsoon . . . . .	266
6.5	Feedback Attributions of Climate Changes Over the South China Sea and Its Adjacent Regions . . . . .	277
6.5.1	Annual Cycles of Surface Temperature . . . . .	277
6.5.2	Interdecadal Change in Troposphere Temperature . . . . .	283
6.6	Uncertainty in Tropical Climate Change Under Global Warming . . . . .	289
6.6.1	Uncertainty in Tropical Rainfall Change . . . . .	289
6.6.2	Uncertainty in Tropical Pacific SST Change . . . . .	292
	References . . . . .	297

**7 Impact of Climate Change Over Southeast Asia and Its Adjacent Regions on Global Climate . . . . . 303**

7.1 Long-Term Trend and Interannual Variation of Springtime Precipitation . . . . . 303

7.2 Effect on East Asian Climate . . . . . 305

7.2.1 Impact of Convection Over the South China Sea and the Philippine Sea on Southern China Precipitation . . . 305

7.2.2 Results from Numerical Model Simulations . . . . . 307

7.3 Influence of Climate Change Over Southeast Asia on Sahel Summer Monsoon Rainfall . . . . . 312

7.3.1 Observed Features . . . . . 314

7.3.2 Numerical Experiments with SAWPSM Latent Heating Anomalies . . . . . 317

7.3.3 Summary and Discussion . . . . . 320

7.4 Impact of Precipitation and Associated Latent Heat Release Over South China Sea and Western Pacific on Global Climate During Boreal Spring and Summer . . . . . 322

7.4.1 Recent Change in Precipitation . . . . . 322

7.4.2 Teleconnection of Precipitation and Atmospheric Circulation Anomaly . . . . . 324

7.4.3 Heating Effect During Boreal Summer . . . . . 330

7.4.4 Heating Effect During Boreal Spring . . . . . 335

7.4.5 Summary and Discussion . . . . . 339

7.5 Impacts of Climate Change in the Central-to-Western Tropical Pacific on Arctic Climate . . . . . 340

7.5.1 Expansion of the Central-Western Pacific Warm Pool Under Global Warming . . . . . 340

7.5.2 Shifting Mode of El Niño in the Contexts of Global Warming and Warm Pool Expansion . . . . . 341

7.5.3 Teleconnection Between Shifting El Niño and Arctic Summer Climate Anomalies . . . . . 343

7.5.4 Convection Differences Associated with Shifting El Niño . . . . . 346

7.5.5 Summary and Discussion . . . . . 348

References . . . . . 350

**8 Subseasonal to Seasonal Prediction of Atmospheric Circulation and Rainfall Over Southeast Asia . . . . . 357**

8.1 Introduction . . . . . 357

8.2 Seasonal Prediction of Atmospheric Circulation and Rainfall Over SEA and Its Adjacent Regions . . . . . 360

8.2.1 Prediction of the Asian Summer Monsoon . . . . . 360

8.2.2 Prediction of the Dominant SST Variability in the Pacific and Indian Oceans . . . . . 362

- 8.2.3 Prediction of the Western Pacific Subtropical High . . . . . 367
- 8.2.4 Prediction of MC Rainfall and Related Atmospheric  
Circulation . . . . . 370
- 8.3 Subseasonal Prediction of Rainfall and Atmospheric Circulation  
in SEA and Its Adjacent Regions . . . . . 380
  - 8.3.1 Subseasonal Prediction of Atmospheric Variability  
Over the Extratropical Northern Hemisphere . . . . . 380
  - 8.3.2 Subseasonal Prediction of the Tropical Climate  
Variability . . . . . 384
  - 8.3.3 Subseasonal Prediction of the Climate Variation  
Over Southeast Asia . . . . . 390
- 8.4 Predictability of Climate Variation Over SEA and Its Adjacent  
Regions . . . . . 397
  - 8.4.1 The Most Predictable Patterns of Rainfall and  
Atmospheric Circulation on Subseasonal and Seasonal  
Scales . . . . . 397
  - 8.4.2 Possible Impact Factors of Seasonal Climate  
Predictability . . . . . 404
  - 8.4.3 Possible Impact Factors of Subseasonal Climate  
Predictability . . . . . 410
- 8.5 Conclusions and Discussion . . . . . 413
- References . . . . . 415

# Chapter 1

## Introduction



Global climate change and its impact are issues concerned gravely by the international community. Under the background of climate change, extreme weather and climate events such as heat waves, droughts, and floods have occurred more and more frequently worldwide, and the impacts of climate change on the human living environment and the development of society and economy have become increasingly significant. Since the United Nations Conference on Environment and Development in 1992, climate change has become the focus of global environmental issues and international political activities. In the past 20 years, the international scientific community has launched several large international research projects such as the World Climate Research Program (WCRP), the International Geosphere-Biosphere Programme (IGBP), the International Human Dimensions Programme on Global Environmental Change (IHDP), the DIVERSITAS projects, and the Global Water System Project (GWSP). The core of these programs is global climate change, especially for the change in physical, chemical, and biological synthesis processes from the interannual, decadal to century time scales and its predictability, as well as the impacts of climate change on the human environment and adaptation policy. In China, the “Twelfth Five-Year Plan for National Economic and Social Development” approved by the 4th Session of the 11th National People’s Congress in 2011 clarified the goals and tasks of China’s economic and social development during the “Twelfth Five-Year Plan” period, in which climate change response as an important content was formally incorporated into the medium- and long-term planning of national economic and social development.

Southeast Asia and its adjacent regions (SAARs) are located in the core of the Asian monsoon system and in the centers of interactions of the Asian monsoon with El Niño–Southern Oscillation (ENSO), the Pacific and Indian Oceans, as well as the Northern and Southern Hemispheres. The SAAR is one of the regions that experiences most pronounced climate change, and is most adversely affected by global climate change. It consists of seas, land, and a group of islands, and its climate is determined by various atmospheric activities on a range of temporal and spatial scales with frequent severe weather and climate events such as typhoons,

heavy rains, droughts, and floods. Meanwhile, the SAAR is characterized by a large amount of latent heat release and is an important heat source of the global atmospheric circulation. The climate change in the SAAR drives the variations of global atmospheric circulation (Webster and Yang 1992), which exerts profound impacts on regional and global weather and climate (Neale and Slingo 2003).

Located to the north of Southeast Asia, China has experienced an increase in the frequency and intensity of extreme weather and climate events under the background of climate change (Herring et al. 2014). Increases in extreme weather and climate events such as heavy rain and flood disasters, typhoons, droughts, and heat waves have led to unprecedented negative consequences for economic and social development and the safety of human lives and properties. Global and regional climate changes have exerted significant effects on China's economic and social development, a major challenge for sustainable development. Previous studies have also shown that the climate change in the SAAR can directly influence China's weather and climate. Therefore, systematical studies of the characteristics and physical mechanisms of the climate change and a better understanding of the climate predictability in the SAAR are not only of great significance to local social and economic development, but also crucial to improved forecast weather and climate in China.

Previous studies of the SAAR climate variability and changes have been mainly focused on winter and summer seasons, with much less attention to spring, the important transitional season from winter to summer. On the one hand, the tropical monsoon, which obtains its maximum intensity in summer, grows rapidly in Southeast Asia during spring, and ENSO events also develop or terminate in (late) spring. The persistent sea surface temperature (SST) anomalies in the tropical Indian Ocean in spring exert a prominent impact on the climate anomalies in the following summer. The tropical and subtropical land surface also warms rapidly and the convective activity over the South China Sea (SCS) warm pool, and the Maritime Continent (MC) grows abruptly in April and May. Moreover, the high-latitude weather systems in the high latitudes often cause significant influences on Southeast Asia in spring. On the other hand, monsoon, ENSO, Indian Ocean SST, land surface processes, and mid-high latitude systems are highly interactive, importantly determining the surface climate anomalies in tropical Asia and surrounding regions in spring and the following summer. Moreover, the western Pacific, the SCS, Southeast Asia, the Qinghai-Tibet Plateau, and the eastern Indian Ocean are the regions significantly sensitive to these ocean-land-atmosphere interactions. Therefore, a profound understanding of the characteristics and mechanisms of climate change in spring and summer in the SAAR under the background of global climate change is undoubtedly important for climate change adaptation in China, Southeast Asia, and other places of the world, improving the ability of climate prediction and the overall capacity of disaster prevention and reduction and promoting the sustainable social development.

This book comprises the following four parts:

**(1) The SAAR climate and its transition between spring and summer under the background of global climate change and impacts on southern China.**

The SAAR links the Indian Ocean and the western Pacific, and is directly adjacent to the regions of South Asian monsoon, East Asian monsoon, and Australian monsoon. Again, it is located in the center of interaction between the East Asian and the Indian monsoon systems and is one of the most active areas of convective heating in Asia. The onset and the intensity of the SCS monsoon directly control the precipitation, droughts, and floods in eastern China. Under the background of global climate change, the changes in large-scale circulation related to tropical monsoons and marine thermal background lead to changes in the SAAR climate and further influence the variability of climate in southern China and even the whole country. Spring is a very important season in seasonal transition, and the climate variability in springtime has a significant impact on the climate in the following summer. The SAARs are sensitive areas for ocean–land–atmosphere interaction during spring and the transition between spring and summer. Compared with winter and summer seasons, there have been much fewer studies on climate change in spring. Under the background of global warming, the SAAR spring climate shows new characteristics, and the key factors that affect the drought and flood disasters in southern China may also change. These changes have increased the difficulty and uncertainty of the prediction of drought and flood disasters, which urgently requires further studies to better understanding the new characteristics and their underlying mechanisms. That is, it is imperative to explore the features, precursors, and mechanisms of the variability and change of the SAAR climate in spring and summer seasons under the global climate change background.

**(2) Impacts of ocean–land–atmosphere interaction over the Tibetan Plateau (TP), Southeast Asia, and the Indian–Pacific regions on the climate in Southeast Asia and China.**

Southeast Asia is characterized by complex topography and land–sea distribution, including the water domains and islands of the MC where ocean–land–atmosphere interaction is particularly active. The TP, the “roof of the world” adjacent to Southeast Asia, is a major heat source for the establishment, development, and maintenance of the Asian summer monsoon (Yanai and Wu 2006). It also influences the variability of atmospheric circulation and precipitation in the SAAR on interannual and interdecadal time scales; and the SST anomalies in the Indo-Pacific region, the dipole oscillations of SST in the equatorial Indian Ocean, and the SST anomalies in the SCS all exert significant effects on Asian monsoon climate. However, it should also be noted that the TP, the East Asian continent, the tropical ocean, and the Asian monsoon are closely interrelated and can be viewed as a complexly integrated “system”. The ocean–land–atmosphere interactions in these areas are specifically important to the climate variability during springtime and the transition between spring and summer, but the physical characteristics and the related dynamic processes, as well as the significance of their role

in understanding and predicting climate variability, are still unclear. Therefore, this monograph is aimed at expanding our understanding of the ocean–land–atmosphere interaction among Southeast Asia, the Indo-Pacific region, the East Asian continent, and the TP on multiple time scales, together with their effects on the global climate, especially during the spring and summer seasons.

**(3) Attribution of SAAR climate change and its uncertainty, feedback of SAAR climate change on the global climate, and connection between regional and global climate changes.**

As part of the SAAR, the Indo-Pacific warm pool is the largest heat reservoir in the world, and the subtle changes in this area can lead to an abnormal climate in adjacent regions and even over the globe. As well known, the changes in the western Pacific warm pool are closely linked to ENSO and its variability. The SCS is located on the western edge of the tropical Pacific Ocean, known as “small warm pool,” along with the Gulf of Mexico which has become one of the hot spots of climate research in the Americas. The thermodynamic and dynamic variability of the SCS is the key to the onset and evolution of the East Asian monsoon, as the Indian Ocean processes determine the onset and intensity of the southwest monsoon, partially through the Somali jet. The exchanges of water and other physical properties among the western Pacific, the SCS, and the Indian Ocean via the Indonesian through flow and other ocean currents affect the onset and evolution of both the East Asian monsoon and the South Asian monsoon, thereby causing abnormal climate in other regions. By applying a climate feedback-response analysis method (Cai and Lu 2009; Lu and Cai 2009), the climate change in the SAAR is systematically attributed to various physical processes, and the different contributions of these physical processes are quantified. In addition, previous studies are mostly concentrated on the impact of global climate change on regional climate, but the feedback of SAAR climate change on the global climate is seldom addressed. This monograph is intended to fill this gap and demonstrate the impact of climate change in Southeast Asia on the climate of South Asia, East Asia, Africa, and even North America. The results discussed are helpful for enhancing our understanding of the link between regional and global climate changes and arousing more attentions of the international community on SAAR climate change.

**(4) Predictability of atmospheric circulation and precipitation in the SAAR on subseasonal-to-seasonal time scales.**

The weather and climate in Southeast Asia are affected by remote atmospheric circulation systems on the one hand, but exert significant influences on the weather and climate in adjacent and remote regions on the other hand. Therefore, the capability of Southeast Asian weather and climate prediction is not only influential on local social and economic development but also essential to the weather and climate prediction in China and other regions. Currently, two major approaches are generally adopted in operational climate prediction: the traditional statistical method and the dynamic prediction method based on the climate system models. With the continuous improvement of high-performance computers and climate system models, the accuracy of the dynamic prediction method has



been constantly improved, e.g., on subseasonal-to-seasonal time scales. Although climate system models can demonstrate their advantages, they also exhibit obvious deficiencies. Therefore, how to extract useful information from model simulations for climate prediction and how to further improve the capabilities of prediction by climate system models are important issues in the areas of climate prediction and model development.

It is worth noticing that most of the contents of this monograph are based on the latest findings from research supported by the National Key Research Program of China under project “Characteristics and mechanisms of climate variability in spring and summer in Southeast Asia and its adjacent regions under the background of global change and its feedback on global climate.” With the latest observation and reanalysis data, state-of-the-art numerical models, and advanced climate dynamic diagnostic methods, the variability and change of SAAR climate in spring and the spring–summer transition period were studied systematically, and a series of new features of the physics and dynamics of SAAR climate were presented. It is anticipated that this book will serve as a starting point of relevant studies and attract more attention to the research of SAAR climate to further enhance our understanding of the long-term change and improve the capacity of prediction of the regional weather and climate.

The publication of this book was supported by the National Key Research Program of China (2014CB953900), the National Natural Science Foundation of China (Grants 41690123, 41690120, 91637208, 41975080, 41975074, and 41805050), and the innovation team of “Ocean–Land–Atmosphere Interaction and Its Global Effects” from the Southern Marine Science and Engineering Guangdong Laboratory (Zhuhai).

This book was mainly completed by Song Yang (Sun Yat-sen University), Renguang Wu (Zhejiang University), Maoqiu Jian (Sun Yat-sen University), Jian Huang (Guangzhou Institute of Tropical and Marine Meteorology, China Meteorological Administration), Xiaoming Hu (Sun Yat-sen University), Ziqian Wang (Sun Yat-sen University), and Xingwen Jiang (Chengdu Institute of Plateau Meteorology, China Meteorological Administration).

A list of the names of contributing authors for individual chapters of this book is provided below:

Chapter 1 (this chapter) Song Yang;

Chapter 2 Maoqiu Jian, Zhiping Wen, Ailan Lin, Dejun Gu, Yunting Qiao, and Chao He;

Chapter 3 Renguang Wu, Jiangyu Mao, Guanghua Chen, Liang Wu, and Wenting Hu, Xi Cao;

Chapter 4 Jian Huang, Qian Li, Zhigang Wei, and Jiangnan Li;

Chapter 5 Ziqian Wang, Wei Wei, Song Yang, and Mengmeng Lu;

Chapter 6 Xiaoming Hu, Yana Li, Song Yang, Ping Huang, Ming Cai, Junwen Chen, Wenshi Lin, and Jun Ying;

Chapter 7 Song Yang, Bian He, Chundi Hu, Zhenning Li, Shan He, and Kaiqiang Deng;

Chapter 8 Xingwen Jiang, Song Yang, Xiangwen Liu, Tuantuan Zhang, and Shaorou Dong.

## References

- Cai M, Lu J (2009) A new framework for isolating individual feedback processes in coupled general circulation climate models. Part II: Method demonstrations and comparisons. *Clim Dyn* 32:887–900. <https://doi.org/10.1007/s00382-008-0424-4>
- Herring SC, Hoerling MP, Peterson TC et al (2014) Explaining extreme events of 2013 from a climate perspective. *Bull Amer Meteor Soc* 95(9):S1–S96
- Lu J, Cai M (2009) A new framework for isolating individual feedback processes in coupled general circulation climate models. Part I: formulation. *Clim Dyn* 32:873–885. <https://doi.org/10.1007/s00382-008-0425-3>
- Neale R, Slingo J (2003) The Maritime Continent and its role in the global climate: a GCM study. *J Climate* 16:834–848
- Webster PJ, Yang S (1992) Monsoon and ENSO: Selectively Interactive Systems. *Q J R Meteorol Soc* 118:877–926. <https://doi.org/10.1002/qj.49711850705>
- Yanai M, Wu GX (2006) Effects of the Tibetan Plateau. In: *The Asian Monsoon*. Springer Praxis Books. Springer, Berlin, Heidelberg. [https://doi.org/10.1007/3-540-37722-0\\_13](https://doi.org/10.1007/3-540-37722-0_13)

## Chapter 2

# Characteristics of the Spring–Summer Atmospheric Circulation Transition Over the South China Sea and Its Surrounding Regions and Their Responses to Global Warming



The South China Sea (SCS) connects the Indian Ocean and the Pacific Ocean. It is also a key region where the East Asian monsoon system and the Indian monsoon system interact with each other, and it is a direct source of moisture for the subtropical monsoon system of East Asia. The onset and intensity of SCS summer monsoon (SCSSM) have great influences on precipitation, which may lead to droughts and floods in southern China in summer. In the context of global warming, the changes in the tropical monsoons on large scale and the marine thermal environment may lead to climate change in the SCS and its surrounding areas, which could exert a significant impact on the climate in southern China.

The transition season usually begins in mid-spring and ends in early summer for the circulation system from a winter pattern to a summer pattern in the Asian monsoon region. In the spring–summer transition stage, the SCS and its surrounding areas are highly sensitive to global air–sea and air–land interactions. Compared with the research on winter and summer seasons, there have been fewer studies on climatic characteristics of spring–summer circulation transition (hereafter, the transition), their variation in the region, and their impact on the summer climate in eastern China. In the context of global warming, the transition over the SCS and its surrounding areas may have some new characters, and the key factors for these new changes and the mechanisms behind them are worth investigating. These changes aggravate the difficulty and uncertainty of drought and flood prediction in southern China. We urgently need to study and understand the physical mechanisms behind the present and future climate changes during spring–summer. Therefore, it is of great significance to study the characteristics and mechanisms of the transition over the SCS and its surrounding areas, and their influences on the climate in southern China under global warming.

In this chapter, the characteristics and physical processes of spring–summer atmospheric circulation transition (hereafter, the transition) over the SCS and its surrounding areas are presented using historical observation data and reanalysis outputs. The effects of tropical intraseasonal oscillation on the onset of the SCSSM are discussed. Precursory signals of sea surface temperature (SST) controlling the

early and late onsets of the SCSSM are also analyzed. Finally, the responses of the transition to greenhouse gas (GHG) forcing in Southeast Asia and its surrounding areas, and the large-scale subtropical anticyclones are studied using the model outputs from the Coupled Model Intercomparison Project Phase 5 (CMIP5).

## 2.1 Characteristics of the Transition Over the SCS and Its Surrounding Regions

The spring–summer transition has always been an important issue for both the academic research community and operational forecasting centers. Yeh et al. (1958) first revealed abrupt changes of the upper atmospheric circulation in the mid- and high latitudes of the Northern Hemisphere in June and October, respectively. Murakami and Nakazawa (1985) investigated the long period of transition from the Southern Hemisphere summer monsoon to Northern Hemisphere summer monsoon, and confirmed the northward migration of low outgoing longwave radiation (OLR) during the transition period. Xie and Sun (1991) emphasized the difference between the transition characteristics of the atmospheric circulation over the Eastern and Western Hemispheres. They considered that the main transition feature of the atmospheric circulation over the Eastern Hemisphere is the establishment of the summer monsoon, which is characterized by three successive phases: moisture slowly increasing, moisture rapidly increasing, and the well-established summer monsoon. Yasunari (1991) found that the interannual variability of the air–ocean–land coupled system over the tropical Pacific and the Asian monsoon regions shows a quasi-biennial nature with the change of sign during the boreal spring to summer, and the concept of “the monsoon year” was proposed as a climate year for the interannual anomalies over the tropics. He et al. (1996) analyzed the seasonal transition features of the Asian summer monsoon (ASM) establishment, and indicated that the transition begins as early as April, followed by abrupt changes in May to June, and the ASM is fully established in June.

The onset of summer monsoon has been considered as an important component of the transition over the monsoon regions. Its mechanism and influence on summer climate have drawn great concerns of researchers domestically and internationally. The transition may have immediate impacts on the summertime occurrence of droughts and floods over Asia (Nitta 1987; Huang 1992; Lau and Yang 1997). An earlier transition may result in an earlier outbreak of southwesterly winds in the low latitudes and more moisture transportation to East Asia, which is conducive to increasing summer precipitation. Therefore, studies on the characteristics of the transition are important for accurate prediction of summer precipitation over East Asia.

In previous studies on the transition, the focus was often on regional summer monsoon. In reality, the onset of summer monsoon occurs in stepwise phases and in different regions (Wang and Lin 2002). The transition has not been adequately understood because of regional distinctions in the summer monsoon regions. In

this respect, several questions we attempt to answer in this chapter are as follows. How to define the spring–summer atmospheric circulation transition? What are the characteristics of the transition? What are the factors responsible for the transition?

### 2.1.1 Characteristics of the Transition

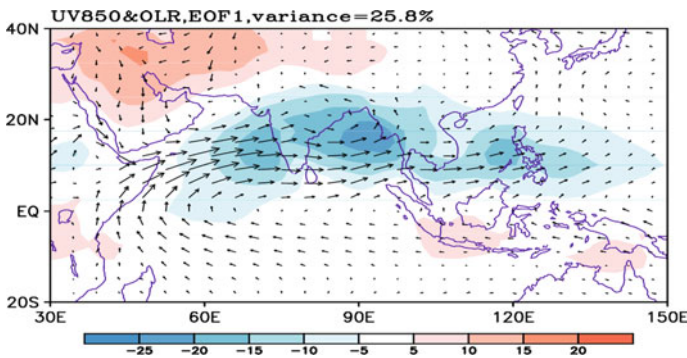
#### (1) Identification of the Transition

In January, a lower-level anticyclone prevails over the Asian monsoon area; meanwhile, the cold air from Mongolia and Siberia moves southward along eastern China into the SCS area, and changes to easterlies over the northern Indian Ocean. In July, the lower-level atmospheric circulation in the Asian monsoon area changes from anticyclonic to cyclonic, with a strong westerly flow over the northern Indian Ocean. In this respect, April–May–June (AMJ) can be considered as a transition season.

In Sect. 2.1, multivariate empirical orthogonal function (MV-EOF) analysis is applied to 5-day running means of OLR and 850-hPa wind from AMJ. The domain of analysis is ( $30^{\circ}$ – $150^{\circ}$  E,  $20^{\circ}$  S– $40^{\circ}$  N) where the ASM is active. The mean state is defined as the climatological AMJ mean, and is subtracted from the data before performing the MV-EOF analysis.

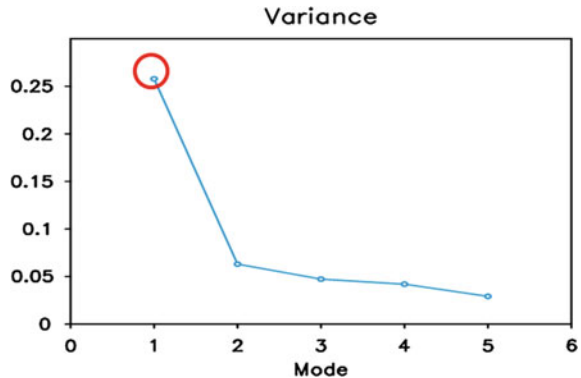
The first MV-EOF mode (Fig. 2.1) shows that the active convections are located over the Arabian Sea (AS), the Bay of Bengal (BOB), and the SCS, while the convections are suppressed over the Arabian Peninsula and the southern Maritime Continent (MC). An anomalous anticyclonic circulation appears over the equatorial Indian Ocean with cross-equatorial flow developing over Somali. The westerlies prevailing in the northern Indian Ocean expand eastward to the SCS, and monsoon troughs develop over the BOB and the SCS.

Figure 2.2 shows a scatter plot of variances explained by the first five modes of the MV-EOF analysis. The first leading mode is statistically distinguishable from



**Fig. 2.1** Spatial pattern of the leading MV-EOF mode of OLR (shading;  $\text{W m}^{-2}$ ) and 850-hPa wind (vector;  $\text{m s}^{-1}$ ) during April–June of 1979–2010

**Fig. 2.2** Explained variances of the first five MV-EOF modes



the other four higher modes according to the rule given in North et al. (1982). Furthermore, the spatial pattern of the first MV-EOF mode of OLR in Fig. 2.1 is similar to the standard deviation of daily OLR for AMJ, especially for the areas of active convections (not shown). The first MV-EOF mode exhibits the transition of the spring–summer atmospheric circulation on a large scale, and its principal component (PC1) is thus useful for identifying the timing of the transition.

## (2) Timing of the Transition

The corresponding PC1 shown in Fig. 2.3 is mostly negative in the early stage, and turns positive in the later stage from April to June. The PC1 value in some of the years rises sharply and changes sign from negative to positive only once, such as in 1989, reflecting a stable transition of the atmospheric circulation from spring to summer. However, in some years the PC1 fluctuates between negative and positive values, such as in 1997, indicating possible impacts of internal atmospheric processes. To identify the date of the transition, we use the following objective criteria.

The transition date is defined as the first day that satisfies the following two criteria: (1) PC1 changes signs from negative to positive and remains positive for at least five days; (2) in the subsequent 20 days (including the transition date), PC1 value must be positive in for least 10 days.

Table 2.1 lists the dates and corresponding pentads of the transition for each year, based on the above definition. The long-term mean transition date (pentad) is May 16 (Pentad 28). The earliest transition occurred on April 25 (Pentad 23) 2008, while the latest was on June 4 (Pentad 31) 1979 and 1992. The maximum range is about 40 days (8 pentads). The long-term mean transition date is close to that of the SCSSM onset.

Seen from the above analysis, the transition is characterized by strong convection over the AS, the BOB, and the SCS, as well as the establishment of 850-hPa westerlies over the northern Indian Ocean. The transition is thus closely related to the onset of the summer monsoon over the AS, the BOB, and the SCS.

Figure 2.4 shows the time series of the transition dates, the BOB summer monsoon (BOBSM) onset dates, the SCSSM onset dates, and the Indian summer monsoon

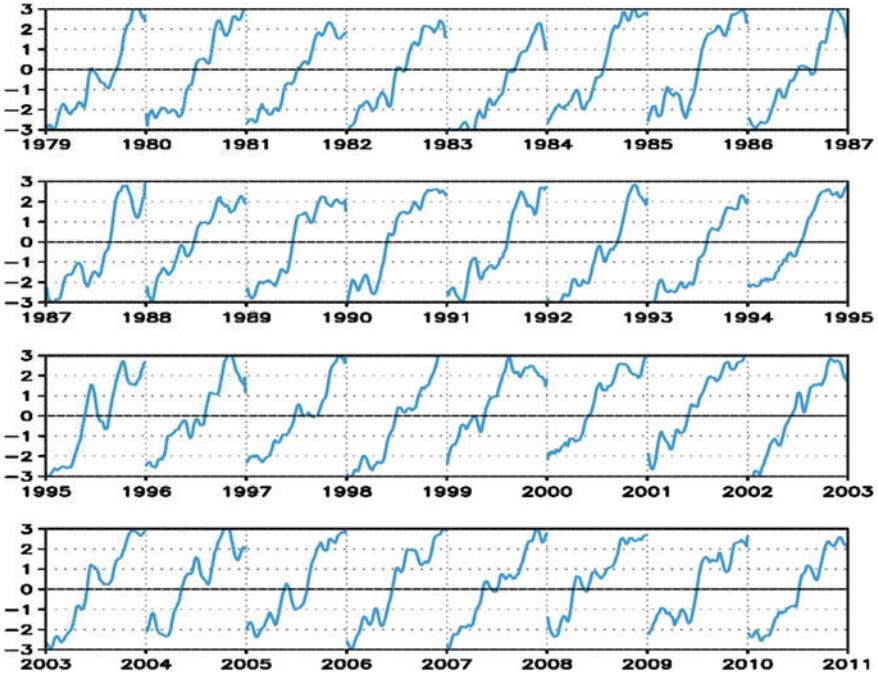


Fig. 2.3 PC1 of the first MV-EOF mode. Only the data from 1 April to 30 June are displayed for each year

(ISM) onset dates. The correlation coefficients of the transition dates with the BOBSM onset dates and the SCSSM onset dates are 0.41 and 0.42, respectively, at the 95% confidence level; and the correlation coefficient between the transition dates and the ISM onset dates is 0.51, at the 99% confidence level. On average, the BOBSM onset is earlier than the transition, the SCSSM onset, and the ISM onset, while the ISM onset is the latest. An interdecadal shift of the SCSSM onset date in the early 1990s is observed. Before the early 1990s, the SCSSM onset is mostly later than the transition date, but it is much closer to the transition date after the early 1990s. These results indicate that the transition, which is characterized by changes in large-scale circulation and convection, is different from the onset of the regional summer monsoon, albeit the two are well correlated.

(3) Evolution of Convection and Atmospheric Circulation during the Transition

To reveal the evolution of convection associated with the transition, we composite the evolution of 10-day-mean OLR based on the transition dates (by centering on the transition day). The transition day is denoted as day 0, while the “-” sign denotes prior to the transition date. The time mean between days -30 and 30 is removed.

During days -30 to -21 (Fig. 2.5, top left panel), three maximum OLR centers (which denote suppressed convection) appear over the AS, the BOB, and the SCS, respectively. The minimum OLR centers (which represent strong convection) cover

**Table 2.1** Dates and pentads of the transition

Year	Date	Pentad	Year (cont'd)	Date (cont'd)	Pentad (cont'd)
1979	6.4	31	1995	5.7	26
1980	5.16	28	1996	5.25	29
1981	5.17	28	1997	5.15	27
1982	5.16	28	1998	5.16	28
1983	6.2	31	1999	5.5	25
1984	5.22	29	2000	5.8	26
1985	5.17	28	2001	5.8	26
1986	5.16	28	2002	5.10	26
1987	5.30	30	2003	5.9	26
1988	5.15	27	2004	5.3	25
1989	5.13	27	2005	5.26	30
1990	5.8	26	2006	5.13	27
1991	5.26	30	2007	5.4	25
1992	6.4	31	2008	4.25	23
1993	5.25	29	2009	5.16	28
1994	5.19	28	2010	5.17	28
			<b>Average</b>	<b>5.16</b>	<b>28</b>

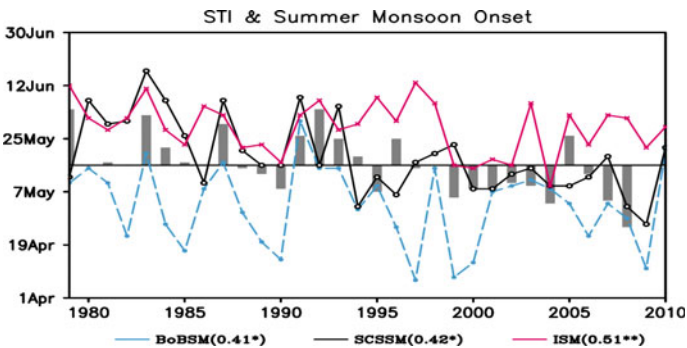


**Fig. 2.4** Time series of the spring–summer atmospheric circulation transition dates (gray bars), the BOBSM onset dates (blue dots; 850-hPa zonal wind averaging over 90°–100° E, 5°–15° N; Mao and Wu 2007), the SCSSM onset dates (black circles; 850-hPa zonal wind averaging over 110°–120° E, 5°–15° N; Kajikawa and Wang 2012), and the ISM onset dates (red crosses; 850-hPa zonal wind averaging over 40°–80° E, 5°–15° N; Wang et al. 2009) for the period 1979–2010. The long-term-mean transition date (May 16) is indicated by a black line. The correlation coefficients of transition dates with BOBSM onset dates, with SCSSM onset dates, and with ISM onset dates are 0.41, 0.42, and 0.51, respectively. Symbols \* and \*\* indicate the 95% and 99% confidence levels, respectively



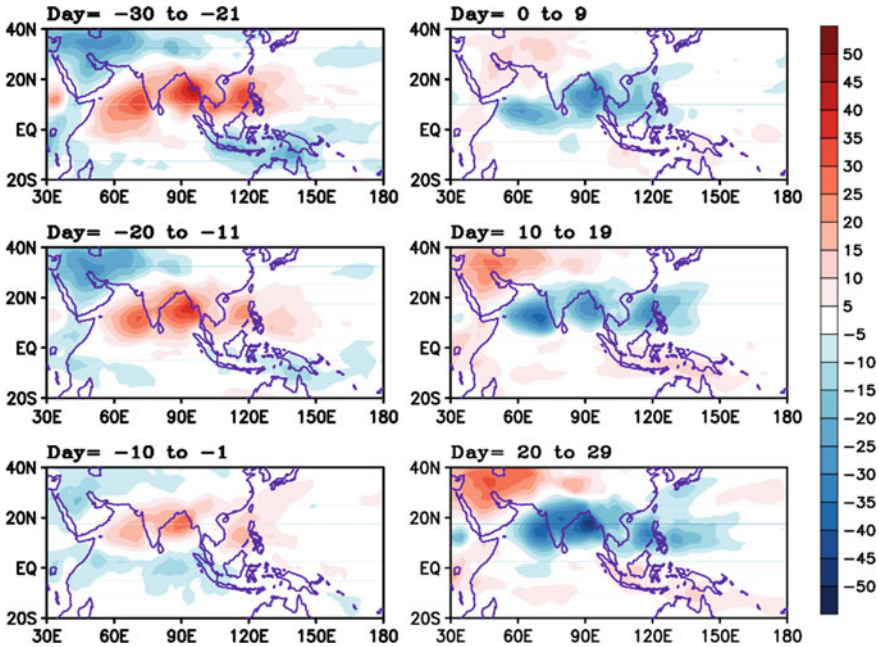
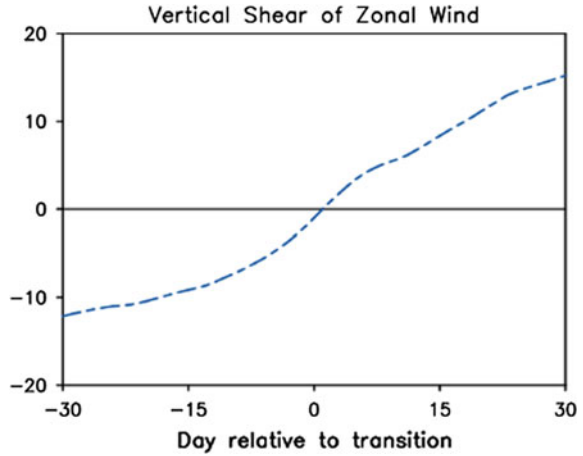


**Fig. 2.5** Composites of 10-day-mean OLR anomalies from days  $-30$  to  $29$ . Note that the time mean between days  $-30$  and  $30$  is removed. Shading interval is  $5 \text{ W m}^{-2}$

the MC. For the next 10 days (days  $-20$  to  $-11$ , Fig. 2.5, middle left panel), the maximum OLR centers are weakened, so are the minimum OLR centers over the MC, while weak convection develops over the southwestern Indian Ocean and extends northeastward. During the period from days  $-10$  to  $-1$  (Fig. 2.5, bottom left panel), the northeastward convection arrives at the equatorial Indian Ocean. The OLR field changes suddenly after the transition. The active convections are located over the AS, the BOB, and the SCS, while the convections are suppressed over the MC. In the ensuing days (Fig. 2.5, right panel), the three minimum OLR centers intensify, reaching the maximum intensity at days  $20-29$ . Meanwhile, the strong convection over the AS and the SCS extends northward and eastward, respectively.

The characteristics of the wind field during the transition are manifested as the changes of vertical shear of zonal wind. Following Webster and Yang (1992), we calculate the area-mean vertical shear of zonal wind between  $850$  and  $200 \text{ hPa}$  in the region of ( $40^\circ-110^\circ \text{ E}$ ,  $0^\circ-20^\circ \text{ N}$ ), and show its evolution during the transition in Fig. 2.6. This region has westerly vertical shear before the transition and reverses to easterly vertical shear after the transition, which is conducive to the development of convection. Thus, the convection and vertical shear of zonal wind change notably during the transition, and their transition times are consistent with each other.

**Fig. 2.6** Time series of area-mean vertical shear of zonal wind (U850 minus U200;  $\text{m s}^{-1}$ ) over ( $40^\circ\text{--}110^\circ\text{ E}$ ,  $0^\circ\text{--}20^\circ\text{ N}$ )



### 2.1.2 Physical Processes of the Transition

To better understand the physical processes associated with the transition, we define the transition pentad as Pentad 0 and regroup the time series of 224 pentad data (seven pentads centered at the transition pentad each year, for a total of 32 years). An MV-EOF analysis is then reapplied to the 224 pentads of OLR and 850-hPa wind. Figures 2.7 and 2.8 show the spatial patterns and principal components of the first and second MV-EOF modes, respectively. The first MV-EOF mode explains 14.9% of the total variance, and the second MV-EOF mode accounts for 10.3% of the total

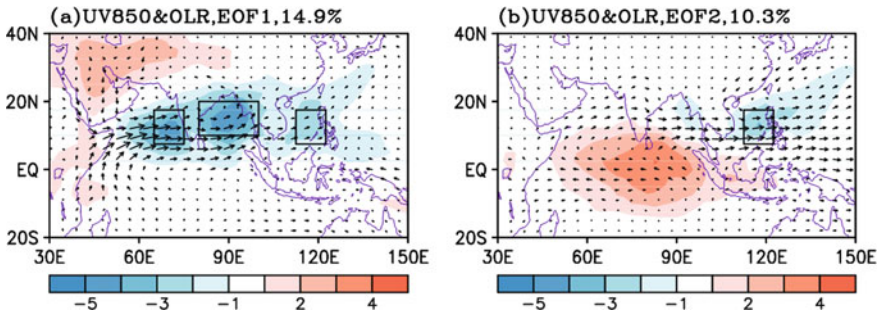


**Fig. 2.7** Spatial patterns of **a** the first and **b** the second MV-EOF modes of the 224 pentads (seven pentads centered at the transition pentad  $\times$  32 years) OLR (shading;  $\text{W m}^{-2}$ ) and 850-hPa wind (vector;  $\text{m s}^{-1}$ ). The boxes in **a** denote the Arabian Sea region ( $65^\circ\text{--}75^\circ\text{ E}$ ,  $7.5^\circ\text{--}17.5^\circ\text{ N}$ ), the Bay of Bengal region ( $80^\circ\text{--}100^\circ\text{ E}$ ,  $10^\circ\text{--}20^\circ\text{ N}$ ), and the South China Sea region ( $112.5^\circ\text{--}122.5^\circ\text{ E}$ ,  $7.5^\circ\text{--}17.5^\circ\text{ N}$ ), respectively. The box in **b** indicates the South China Sea region only

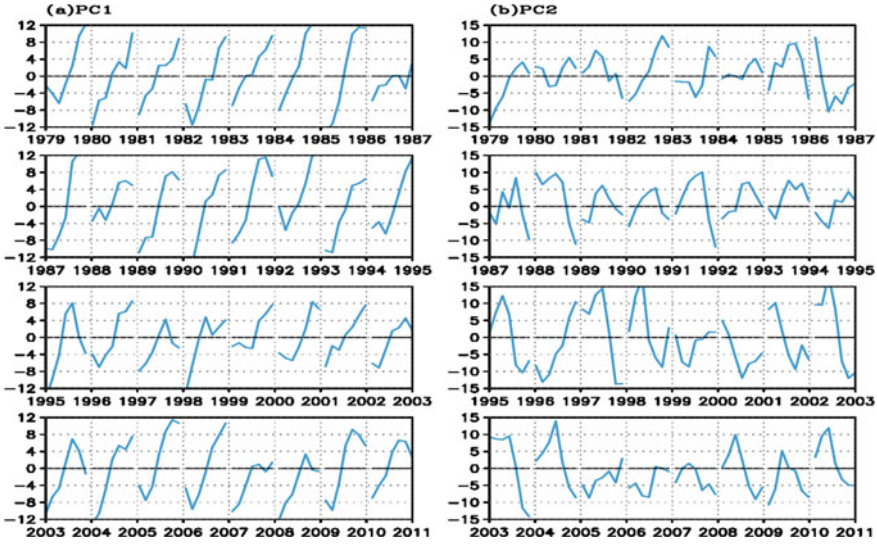


**Fig. 2.8** a PC1 and b PC2 of the MV-EOF modes in Fig. 2.7. Only the data from the seven pentads centered at the onset are displayed for each year

variance. Compared with the daily MV-EOF modes shown in Fig. 2.1, the pentad modes depict similar spatial patterns, except for a weaker OLR center over the SCS.

Table 2.2 presents the correlation coefficients of PC1 and PC2 with OLR in the AS region (65°–75° E, 7.5°–17.5° N), the BOB region (80°–100° E, 10°–20° N), and the SCS region (112.5°–122.5° E, 7.5°–17.5° N), respectively. We can see that PC1 is highly correlated with the OLR in the three key regions. The correlation coefficients are as high as 0.78, 0.86, and 0.54, respectively, and are all significant at the 99% confidence level. In contrast, PC2 has a weak correlation with the OLR in the three key regions. The correlation coefficient between PC2 and OLR in the SCS region only reaches 0.52, comparable to that of PC1 with OLR in the same region. The other two have weak correlations. Therefore, the first MV-EOF mode is indicative of the evolution of the convection over the AS and the BOB during the transition, while both the first and second MV-EOF modes are needed to explain the convection over the SCS.

**Table 2.2** Correlation coefficients of PC1 and PC2 with OLR in the three regions shown in Fig. 2.7a. OLR is multiplied by -1

	OLR-AS	OLR-BOB	OLR-SCS
PC1	0.78**	0.86**	0.54**
PC2	-0.27	0.09	0.52**

\*\*Indicates the correlation is confident at the 99% level. AS: the Arabian Sea; BOB: the Bay of Bengal; and SCS: the South China Sea

## (1) Large-Scale Circulation Transition Mode and Its Evolution

Let us define the first MV-EOF mode, shown in Figs. 2.7a and 2.8a, as large-scale circulation transition mode. To examine the evolution of the OLR in the three key regions before, during, and after the transition stage, we follow the method in Wu and Chou (2012) by calculating the lagged regression of the OLR of each grid box against PC1.

The evolution of OLR consists of three stages (Fig. 2.9). (a) Gestational stage (Pentads  $-10$  to  $-7$ ). At Pentad  $-10$ , the convection occurs over the southern tip of the Indian subcontinent, the Indochinese Peninsula, and the African continent. Then, the convection over the southern tip of the Indian subcontinent strengthens and moves eastward to the southeast of the BOB, merging with the convection over the Indochinese Peninsula. The convection over the African continent develops locally. (b) Developing stage (Pentads  $-6$  to  $-3$ ). From Pentads  $-6$  to  $-3$ , weak convection appears over the SCS and then strengthens locally, as well as the convection over the southeast of the BOB. Meanwhile, the convection over the African continent moves eastward to the western equatorial Indian Ocean. (c) Booming stage (Pentads  $-2$  to  $+1$ ). At Pentad  $-2$ , the convection over the southeast of the BOB flares up and extends eastward to the southern SCS, and the convection over the western Indian

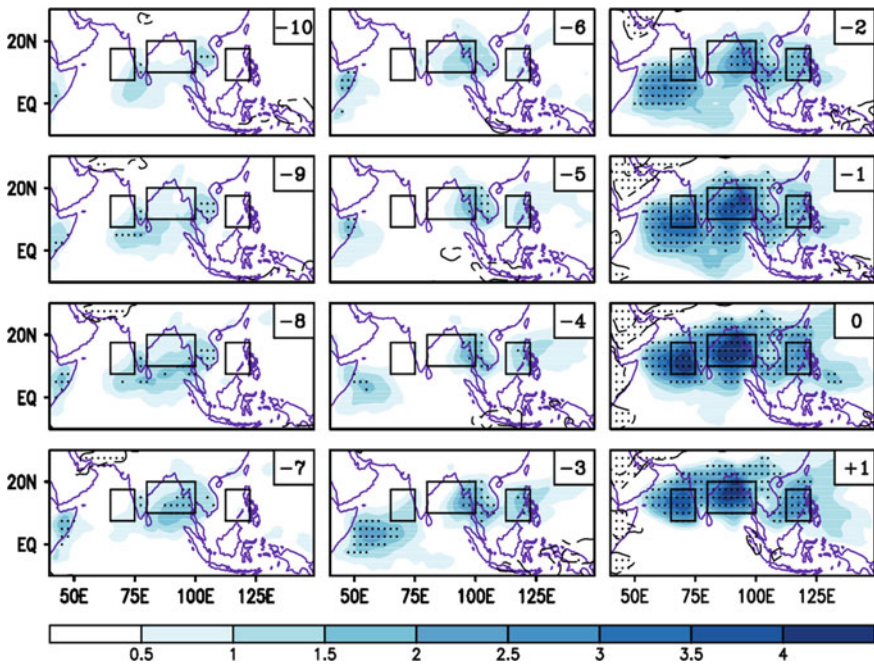


**Fig. 2.9** Lagged regression of OLR ( $\text{W m}^{-2}$ ) against PC1. Negative lag denotes the latter lags the former. Stippling indicates the 95% confidence level

Ocean moves northward to the southeastern AS. From Pentads  $-1$  to  $0$ , the convection over the BOB flares up and extends westward, merging with the convection over the AS. Strong convections cover a large area from the BOB to the AS. By Pentad  $0$ , the OLR centers over the AS, the BOB, and the SCS develop into their maxima, with the centers over the northern Indian Ocean being stronger than the one over the SCS. At Pentad  $+1$ , the convections are separated by the Indochinese Peninsula into two parts and weakened, and the western convection advances northward.

#### (a) Gestational Stage

Warm SST has a major effect on the development of convection. The necessary condition for deep convection can be achieved by SST greater than  $28\text{ }^{\circ}\text{C}$  in combination with some other factors (Fu et al. 1994). Wu et al. (2012) found that a warm pool (SST  $> 30.5\text{ }^{\circ}\text{C}$ ) often occurs in the eastern part of the central BOB before the formation of the BOB monsoon vortex. To investigate the relationship between convection and warm SST during the gestational stage, we show pentad-mean evolution of SST from Pentads  $-10$  to  $-7$  prior to the transition (Fig. 2.10, left panels). We can see that a warm pool (SST  $> 29\text{ }^{\circ}\text{C}$ ) exists over the Indian Ocean, where SST is the highest near the equator and decreases toward higher latitudes. As time progresses, the area of the warm SST expands and moves slightly northward, which is conducive to the formation of convection over the southern Indian subcontinent (Fig. 2.9, left panels). Figure 2.10 (right panels) shows the differences of SST between consecutive pentads. SST increases in the northern tropical Indian Ocean and decreases in the southern tropical Indian Ocean, which coincides with the northward movement of the Sun during the spring–summer seasons. From Pentads  $-9$  to  $-7$ , the increasing SST in the BOB is conducive to the development of convection in this area (Fig. 2.9). Moreover, the SST in the SCS warms up significantly at Pentad  $-7$ , which may play an important role in maintaining the convective activities in subsequent pentads. Therefore, warm SST is the main factor for the formation of convection during the gestational stage.

#### (b) Developing Stage

Figure 2.11 shows the lagged regressions of SST against PC1 from Pentad  $-6$  to  $-3$ . There is a significant positive correlation between convection and SST in the SCS and SST in the ocean east of the Philippines (the boxes shown in Fig. 2.11). Anomalous heating due to warm SST anomalies (SSTAs) in the SCS and in the ocean east of the Philippines induces the cyclonic wind anomalies over the BOB and the SCS via a Rossby wave-type response (Gill 1980), which leads to the development of convection in this area (Fig. 2.9).

#### (c) Booming Stage

High correlations between convection and SST are observed during the gestational stage and the developing stage, but not in the booming stage when the relationship between convection and SST is weakened. Figure 2.12 shows the lagged regressions

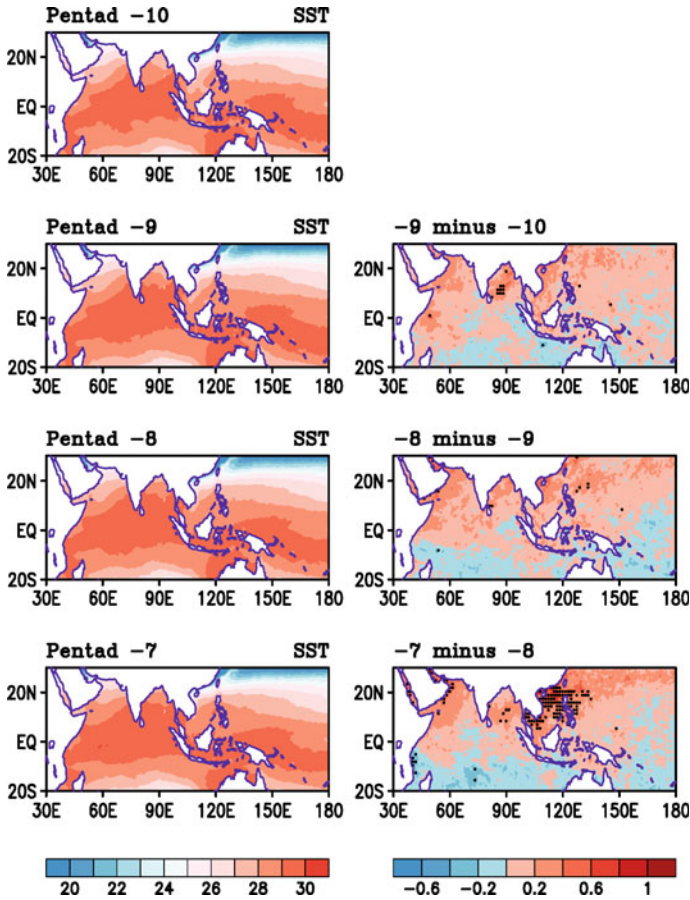


**Fig. 2.10** Pentad means of (left) SST ( $^{\circ}\text{C}$ ) and (right) difference between consecutive pentads. Results are 32-year composites. Stippling indicates the difference is significant at the 95% confidence level

of SST against PC1 from Pentads  $-2$  to  $+1$ . Cold SSTAs appear in the western equatorial Indian Ocean and extend northeastward, while warm SSTAs appear in the subtropical Northwest Pacific. At Pentad  $+1$ , significant cold SSTAs emerge in the southern AS and southern BOB, while the changes of SSTAs in the SCS slow down. This suggests that no striking warming occurs in the southern AS, the southern BOB, and the southern SCS during the booming stage. Deep convection is active regardless of low SST, which indicates that the SSTAs are not a forcing for the transition, but are a response to deep convection development during the booming stage.

Liu et al. (2014a, b) showed that the sensible heat flux is important for atmospheric circulation. The sensible heat flux from the sea surface can generate available potential energy (APE) efficiently in a region where heating and temperature are positively correlated. It can act as a trigger to release positive convective APE (CAPE) in the